

Cranial window implantation on mouse cortex to study microvascular change induced by cocaine

Kicheon Park, Jiang You, Congwu Du, Yingtian Pan

Department of Biomedical Engineering, Stony Brook University, Stony Brook, NY 11794, USA

Correspondence to: Yingtian Pan, PhD, Professor. Department of Biomedical Engineering, State University of New York at Stony Brook, Bioengineering Bldg., Rm. G17, Stony Brook, NY 11794-5281, USA. Email: yingtian.pan@sunysb.edu.

Abstract: Cocaine-induced stroke is among the most serious medical complications associated with cocaine's abuse. However, the extent to which chronic cocaine may induce silent microischemia predisposing the cerebral tissue to neurotoxicity has not been investigated; in part, because of limitations of current neuroimaging tools, that is, lack of high spatiotemporal resolution and sensitivity to simultaneously measure cerebral blood flow (CBF) in vessels of different calibers quantitatively and over a large field of view (FOV). Optical coherence tomography (OCT) technique allows us to image three dimensional (3D) cerebrovascular network (including artery, vein, and capillary), and provides high resolution angiography of the cerebral vasculature and quantitative CBF velocity (CBFv) within the individual vessels in the network. In order to monitor the neurovascular changes from an *in vivo* brain along with the chronic cocaine exposure, we have developed an approach of implanting a cranial window on mouse brain to achieve long-term cortical imaging. The cranial window was implanted on sensorimotor cortex area in two animal groups, i.e., control group [saline treatment, ~0.1 cc/10 g/day, intraperitoneal injection (i.p.)] and chronic cocaine group (cocaine treatment, 30 mg/kg/day i.p.). After implantation, the cortex of individual animal was periodically imaged by OCT and stereoscope to provide angiography and quantitative CBFv of the cerebral vascular network, as well as the surface imaging of the brain. We have observed vascular hemodynamic changes (i.e., CBFv changes) induced by the cranial preparation in both animal groups, including the inflammatory response of brain shortly after the surgery (i.e., <5 days) followed by wound-healing process (i.e., >5 days) in the brain. Importantly, by comparing with the control animals, the surgical-related vascular physiology changes in the cortex can be calibrated, so that the cocaine-induced hemodynamic changes in the neurovasculature can be determined in the cocaine animals. Our results demonstrate that this methodology can be used to explore the neurovascular functional changes induced by the brain diseases such as drug addiction.

Keywords: Cranial window implantation; long-term optical imaging; optical coherence tomography (OCT); vascular network; cerebral blood flow (CBF)

Submitted Oct 21, 2014. Accepted for publication Oct 31, 2014.

doi: 10.3978/j.issn.2223-4292.2014.11.31

View this article at: <http://dx.doi.org/10.3978/j.issn.2223-4292.2014.11.31>

Introduction

Cocaine abuse increase the risk of life-threatening neurological complications, e.g., strokes, seizures and transient ischemic attacks. About 25–60% of cocaine-induced stroke can be attributed to cerebral vasospasm and ischemia (1-4). Previous human magnetic resonance imaging (MRI) and positron emission tomography (PET) studies have shown

reduced cerebral blood flow (CBF) in cocaine abusers (5). However, the mechanisms associated with cocaine-induced CBF reduction and cerebral vasospasm and ischemia are not well understood, which may result from the direct vasoconstrictive properties of cocaine.

Despite imaging technology has profoundly advanced our understanding of mechanisms that underlie cocaine

addiction in animals and humans, studies on the vasoactive effects of cocaine in animal models have been hindered by the technical limitations of current neuroimaging techniques. Conventional techniques [e.g., MRI, computed tomography (CT) angiography] fail to provide sufficient spatiotemporal resolutions to measure rapid CBF changes in small vessel compartments (6). While multiphoton microscopy (MPM) (7-9) can detect capillary CBF, its small field of view (FOV) restricts its use for assessing cocaine's cerebrovascular network effects, and it may not be suitable for repeated imaging of disease progression (10) or the dynamics to cocaine responses (e.g., due to complications associated with exogenous fluorescence dye loading and clearance). Recent advances in optical coherence angiography (OCA) (11-14) have markedly improved *in vivo* visualization of the microvascular networks (15,16). Currently, we developed a novel optical imaging technique that allowed us to image three dimensional (3D) capillary cerebrovascular networks quantitatively and at ultrahigh spatial resolution. Specifically, we combined ultrahigh-resolution OCA (μ OCA) (17,18) to enable visualization of capillary cerebrovascular networks, and a new phase-intensity-mapping (PIM) algorithm to optimize the detection sensitivity of ultrahigh-resolution optical Doppler tomography (μ ODT). Additionally, this technique allowed separation of arterial and venous branches and thus characterization of their differences in response to stimuli (e.g., cocaine).

To access the cortical tissue with optical imaging techniques, a cranial preparation could be involved including a thinned skull or window implantation (7,19-21). While thinning skull reduces the scattering and absorption effects on the imaging quality, in the cranial window preparation the skull is completely removed in the window area, and the cortex is exposed to allow directly access the brain tissue for imaging with presumably better resolution. This is important for some studies, especially related to image the microvasculature (e.g., capillaries) to characterize its functional and physiological changes induced by drug (e.g., stimulants such as cocaine) or in the disease brain.

To achieve the ability of imaging the brain for long term, a cranial window implants in the animal are becoming a preparation of choice for stable optical access to the large area of the cortex over extended period of time. In our case here, for example, it is to monitor the potential changes in vascular morphology and/or CBF of the cortex along with the chronic cocaine treatment to the animal. Indeed, it is a challenge to maintain a clear, unobstructed view of the

cortex because the implantation preparation would evoke an inflammatory response, and the detailed dynamics of the response on a chronic timescale, so-called as 'wound healing response', has not been characterized. Therefore, it is not clear how this complex induced by the cranial window preparation would effect on the image of the neurovascular changes induced by cocaine in the brain. The goals of this study are to characterize vascular morphological (represented by OCA imaging) and functional [reflected by CBF velocity (CBFv) obtained from ODT imaging] changes associated with cranial window implantation. We hypothesize the vascular changes induced by the cranial preparation would appear in the cranial widow implanted of the cortex not just in the control mouse but also in the mouse with chronic cocaine exposure. However, we anticipate that the vascular physiological changes in the cortex induced by the window preparation can be calibrated with the control animals, and the cocaine-induced hemodynamic changes in the neurovasculature can be determined accordingly in the cocaine animals.

Materials and methods

Animals

B6 mice (8-week-old male) were used for this study. In each animal, the cranial optical window was implanted on the area of the sensorimotor cortex. After the surgery, the animals were divided into two groups: Group #1 was a control group in which the mice were daily treated with saline; Group #2 was an experimental group in which the mice were daily treated by cocaine. The animal protocols were approved by Institutional Animal Care and Use Committees of Stony Brook University and followed the National Institutes of Health (NIH) Guideline for Care and Use of Laboratory Animals.

Surgery

All surgical devices were pre-sterilized. The mouse was anesthetized with mixture of pure oxygen and 2.0-2.5% of isoflurane. The hair on the mouse head was shaved from near-by eye to the back head by using a small animal trimmer (Model No 41591-04302, Wahl). After stabilizing the animal head on a customized stereotaxic frame, the shaved head area was sterilized with 70% alcohol and povidone-iodine (NDC52380-1855-2, Aplicare Inc.) (Figure 1A) and the skin of ~1 cm in diameter on the cortex

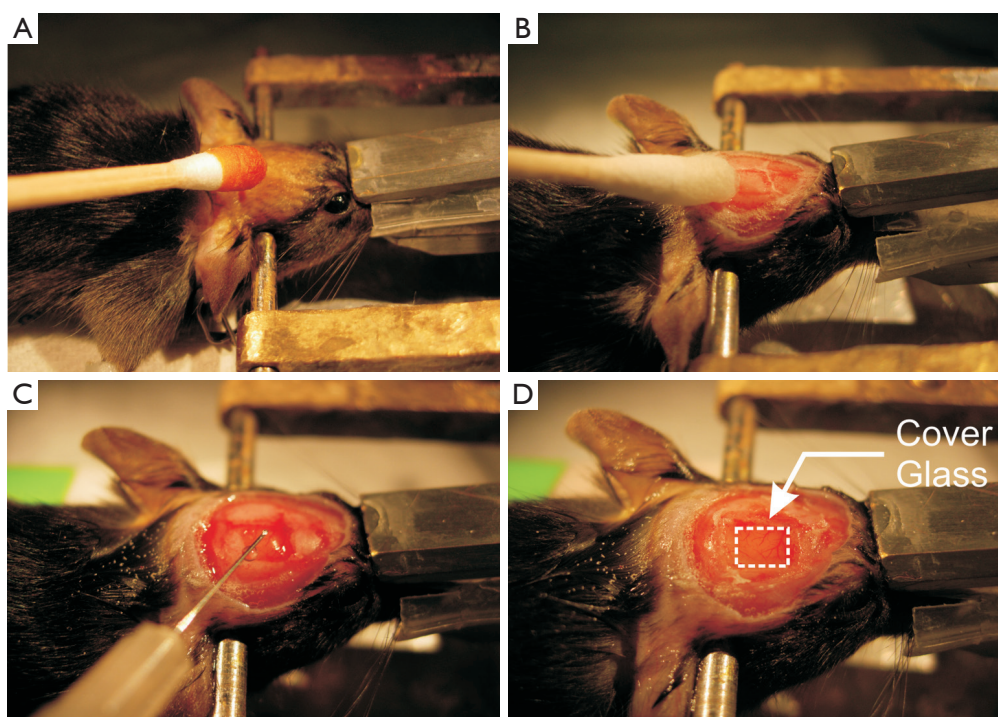


Figure 1 Surgical procedure of cranial window implantation. (A) The mouse head was shaved and fixed on stereotaxic frame and then the skin surface was sterilized with 70% alcohol and povidone-iodine; (B) skin was removed on the head and the tissue on skull was clean with hydro-dioxide; (C) the target area was gently thinned with a dental drill and the Immunosuppressive drugs was applied on brain surface; (D) cover glass was put on the craniotomy and the instant glue was applied on the skull around the craniotomy and dental cement was applied surround the glass on skull.

was cut-off by a scissor and the extra tissue on the skull was removed with hydro dioxide solution (NDC10565-001-04, Hydrox) with a rubbing q-tips (Cat. No. 8884541300, Covidien) (Figure 1B). The skull was then further cleaned with the dry q-tips to explore the positions of begma and lamda that was used as the localization landmarks. A region of interest (ROI), i.e., ROI around lateral: from 0.25 to 2.75 and anterior: from -0.25 to -2.75 was selected on the sensorimotor cortex (Figure 1C) (22,23). Using a dental drill (Ideal micro drill; Roboz) with 0.8 mm drill bit (Part No 60-1000, CellPoint Scientific, Ideal micro-drill burr set), a rectangular region in the skull, i.e., ~2.5 mm × 2.5 mm ROI shown in Figure 1C on the sensorimotor cortex, was thinned and the bone at that brain region was then carefully removed, leaving the dura intact. During the drilling procedure, the drill bit was gently touched to the skull and the cold saline was applied on the operating area within each 10 seconds to prevent from a potential heating effect on the brain that was generated during the drilling process. As illustrated in Figure 1C, an “immunosuppressive drugs”

(dexamethasone sodium phosphate) was then applied on the brain top and the explored brain region was immediately covered by a 4×3 mm² coverslip which was cut 22×50 mm² (Micro cover glasses VWR, Cat. No. 48393059) with carbide scribe (Ted Pella Inc., Fisher Scientific, Cat. No. NC0627043) and sealed with instant glue (Super Glue 3 g, Gorilla Glue Company) (Figure 1D). Dental cement was spread around the edge of the coverslip to further secure its attachment with the skull.

Post-operative care and chronic drug treatment

After the cranial window implantation, the animal was under the post-operative care for 2 days for surgical recovering, including antibiotic and anti-inflammation treatments if necessary. From third day of the surgery, the control group (i.e., Group #1) was administrated with saline [-0.1 cc/10 g/day, intraperitoneal injection (i.p.)], whereas the chronic cocaine group (i.e., Group #2) was administrated with cocaine (30 mg/kg/day i.p.) for consecutive over 27 days.

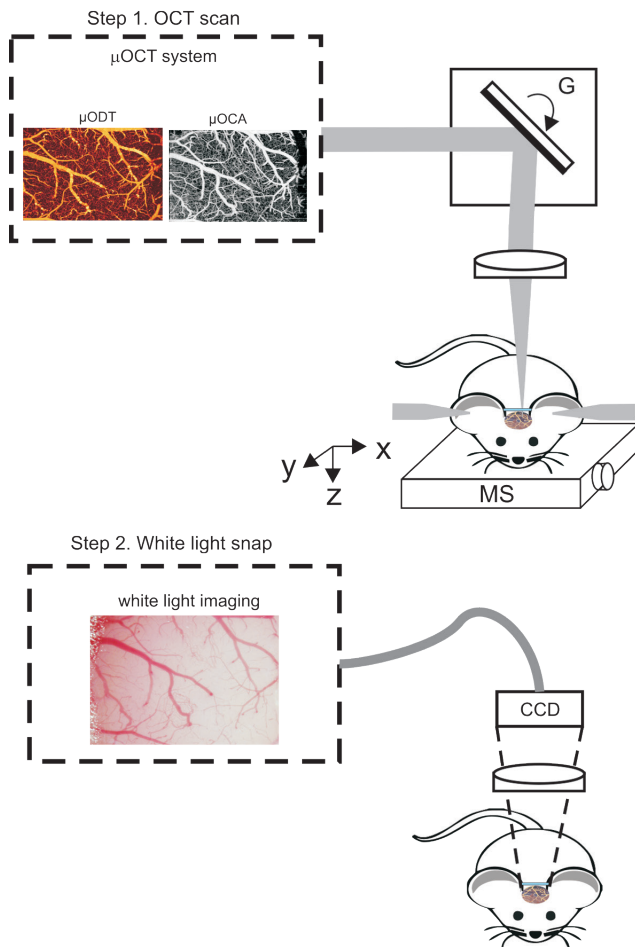


Figure 2 A schematic of hybrid imaging system for ultrahigh-resolution optical coherence tomography (μ OCT) and white light imaging. μ OCT can provide the quantitative ultrahigh-resolution optical Doppler tomography (μ ODT) to image the cerebral blood flow velocity (CBFv) in the cortical vascular network. In addition, it can simultaneously provide the ultrahigh-resolution optical coherence angiography (μ OCA) of the vascular network of cortex as well. The white light imaging modality provides the superficial imaging of the brain surface through the optical window. G, galvo scanning mirrors; MS, motor stage; CCD, charge coupled device.

Neurovascular imaging of *in vivo* brain

From the surgical day on, the mouse brain was imaged through cranial window. By using ultrahigh-resolution optical coherence tomography (μ OCT) the quantitative CBFv by μ ODT was acquired as well as the μ OCA imaging of the cerebral vascular network. Afterwards, the brain surface under the cranial window was imaged by using a stereoscope. Every 3-4 days, these images were taken

repeatedly. In each imaging day, the animal was anesthetized with mixture of oxygen with 1.5-2.0% of isflurane and its head was stabilized by home-modified stereotactic frame for minimizing the motion artifact effect on the imaging. Animal's brain was set to similar angle respect to incident light beam and similar area of sensorimotor cortex to keep the imaging consistency among scans on different day. During the imaging, the physiology of the animal was continuously monitored, including the electrocardiograph (ECG), respiration and body temperature (Model No. 1025T, SA instrumentation).

As illustrated in *Figure 2* a custom spectral domain μ OCT (24) system was used to track cerebral vasculature and CBFv change by post-reconstructed μ OCA (12,25) and μ ODT (26), respectively. The μ OCT system provided axial resolution of $\sim 1.8 \mu\text{m}$ in brain tissue determined by the short coherence length $\{L_c = 2 \ln[2] \lambda^2 / (\pi \Delta \lambda_{\text{FWHM}})\}$, $\Delta \lambda_{\text{FWHM}} \approx 154 \text{ nm}$ —bandwidth of cross-spectrum} and lateral resolution of $\sim 3 \mu\text{m}$ attributed by the numerical aperture (NA) of microscopic objective (f 16 mm/NA0.25). After the μ OCT scan, animal was moved to a stereoscope (Nikon SMZ 1500 with Olympus DP72 Camera) for the white light imaging of brain surface.

Quantification of CBFv change by μ ODT

To quantify the CBFv of heterogeneous flow speed in different types of vessel (i.e., artery, vein, capillary), μ ODT were scanned and reconstructed at two different A-scan frequencies, i.e., 27 kHz and 5 kHz (binning at every two A-line of original 10 kHz scan image). While, in case of 5 kHz scan scheme, the sensitive of slow flow (i.e., flow in capillary) was very high but fast flow rate in large vessel, especially in main artery branch, could be easily saturated. On the contrary, 27 kHz scan scheme was less sensitive for capillary flow while it circumvented phase saturation that easily occurred in slow scan scheme i.e., 5 kHz. Combining these two scan schemes, we enabled to quantify the CBFv in the large vessels (i.e., pial artery and vein) as well as the CBFv in the capillaries.

To calculate the CBFv change [i.e., $\Delta \text{CBFv} (\%)$], CBFv at a selected vessel at a certain day [e.g., t_d , i.e., $\text{CBFv} (t_d)$] was compared with its baseline [i.e., $\text{CBFv} (t_0)$] obtained at the surgical day of the window implantation i.e., $\Delta \text{CBFv} (\%) = \{[\text{CBFv} (t_d) - \text{CBFv} (t_0)] / \text{CBFv} (t_0)\} \times 100$. More than three ROIs for each vessel were selected to calculate its mean $\Delta \text{CBFv} (\%)$ with its standard deviation. To track the capillary $\Delta \text{CBFv} (\%)$ as a function of time, 10 ROIs in

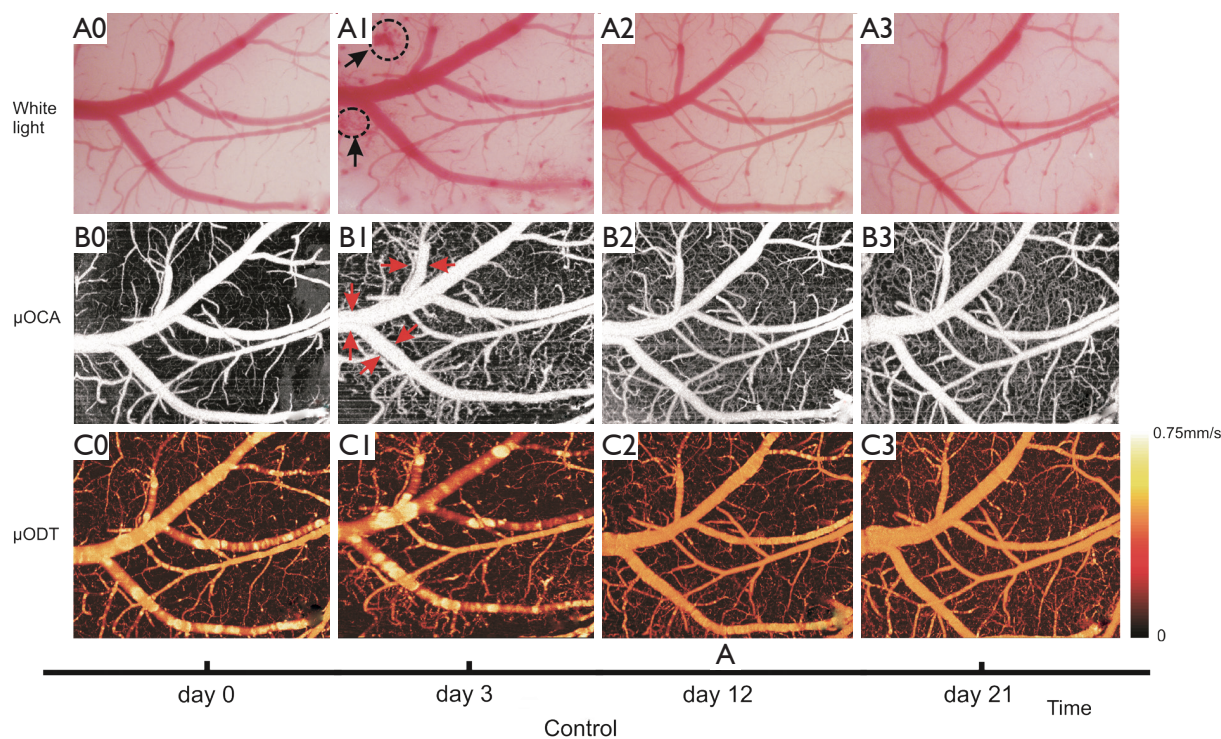


Figure 3 Transformation of a control group animal brain was tracked for 27 days and its representation in day 0, day 3, day 12 and day 21 after the cranial optical window implantation. Row A (i.e., A0-A3), white light image shows the surface image of the cortical brain under the optical window; row B (i.e., B0-B3), ultrahigh-resolution optical coherence angiography (μ OCA) of the vascular network of cortex; row C (i.e., C0-C3), quantitative cerebral blood flow velocity (CBFv) in the cortical vascular network imaged by ultrahigh-resolution optical Doppler tomography (μ ODT). It illustrates the minor bleeding appeared on day 3 (black circle in A1) along with the vessel dilations (red arrows in B1), thus suggesting that the minor bleeding was associated with the hyperemia. The bleeding was recovered afterwards, indicating that it was temporal which might be associated with the local inflammatory response to the surgery (i.e., window implantation). In addition, the CBFv was obviously increased as a function of time, e.g., day 12 (C2) and day 21 (C3) if comparing with day 3 (C1).

capillary bed were selected from the 5 kHz μ ODT imaging and the mean velocity change in capillary Δ CBFv can be determined accordingly from day 0 to day 27 of the cranial window implantation. In order to extract cocaine effect from the wound healing process from brain surgery, we calculated the ratio of Δ CBFv between the cocaine group and the control group and presented the relative changes of mean Δ CBFv over the baseline.

Results

Cortical neurovascular images of in vivo brain through the cranial window

Figure 2 illustrates the systematic set-up for cortical brain imaging from the *in vivo* mouse. The stereoscope is a conventional modality that enables detection of the

reflected light from the brain surface to provide the global view of the cortical brain. By using our home-built μ OCT, we can acquire 3D cross-sectional images of cortical brain structures characterized by their backscattering properties at near real time and over a large FOV (for example, $2 \times 2 \times 1 \text{ mm}^3$) through the cranial window. With the post-image processing algorithms (12,13,27), μ OCT can produce the μ OCA to visualize the vascular networks of cortex. Meanwhile, it can simultaneously measure the flow rates of the blood in the vessels, thus providing the quantitative map of the CBFv in neurovasculature of the brain.

Monitoring vasculature changes as a function of time

Figure 3 represents the repeated images of the same cortical area of a control mouse (i.e., from Group #1) through the

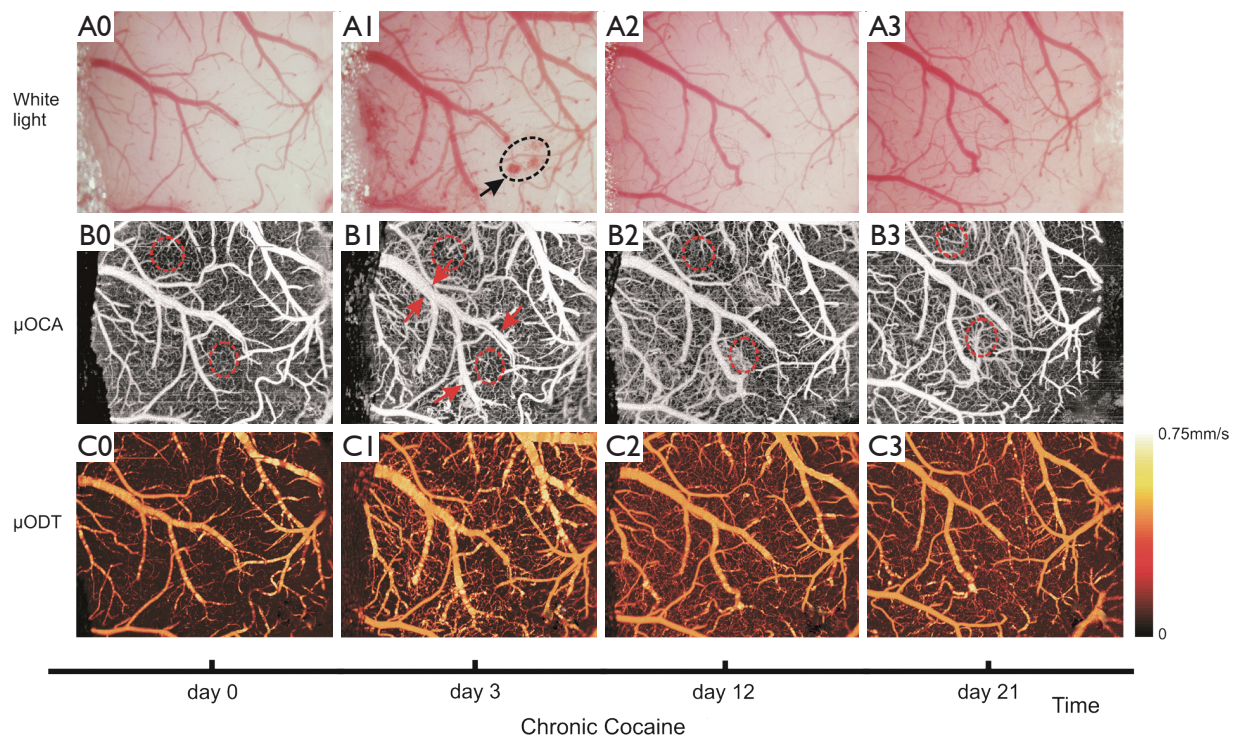


Figure 4 Transformation of a chronic cocaine group animal brain was tracked for 27 days and its representation in day 0, day 3, day 12 and day 21 after the cranial optical window implantation. Row A (i.e., A0-A3), white light image shows the surface image of the cortical brain under the optical window; row B (i.e., B0-B3), ultrahigh-resolution optical coherence angiography (μ OCA) of the vascular network of cortex; row C (i.e., C0-C3), quantitative cerebral blood flow velocity (CBFv) in the cortical vascular network imaged by ultrahigh-resolution optical Doppler tomography (μ ODT). It illustrates the minor bleeding also appeared on day 3 (black circle in A1) along with the vessel dilations (red arrows in B1), thus suggesting that the minor bleeding was associated with the hyperemia. The bleeding was recovered afterwards, indicating that it was temporal which might be associated with the local inflammatory response to the surgery (i.e., window implantation). In addition, the CBFv was not obviously increased as a function of e.g., day 12 (C2) and day 21 (C3) if comparing with day 3 (C1).

cranial window at the implanted day (i.e., day 0), and after implantation at the 3rd day (i.e., day 3), 12th day (i.e., day 12) and 21st day (i.e., day 21), respectively, which includes the reflected white-light image of the cortical surface (i.e., top row A0-A3, Figure 3), the angiography of cortical vascular network (i.e., middle row B0-B3, Figure 3) and the CBFv map of these vessels (i.e., bottom row C0-C3, Figure 3). As shown in Figure 3A0-A3 the reflected-white light images of the brain seems no significant change over the 21 days except that a very small bleeding spots were observed on the day 3 (i.e., black circle, Figure 3A1). Interestingly, the angiography image shows that the vascular network was intact at those location (i.e., Figure 3B1), however, the vessel dilation was observed on day 3 after the window implantation (red arrows, Figure 3B1) if comparing with its baseline (i.e., day 0, Figure 3B0), which indicates that

the hyperemia induced on day 3 might induce the surface microvascular burst and result in the local small bleeding. It should be noted that the bleeding spots were disappeared after day 7 as shown in Figure 3A2 and the diameters of major vessels tended to be returned to the normal sizes in the baseline (Figure 3B2). This indicates that the bleeding of the microvascular around day 3 was temporal and the vascular dilatation might reflect the inflammatory response to the surgery in the brain.

Figure 4 shows the cortical images of a cocaine mouse from the Group #2, which was administered with cocaine daily (30 mg/kg/day, i.p.) for consecutive 27 days and the images was taken repeatedly on the certain days during the treatment period from the same area of the cortex through the cranial window. As shown in Figure 4A1, a microvascular bleeding was also observed on day 3 (black

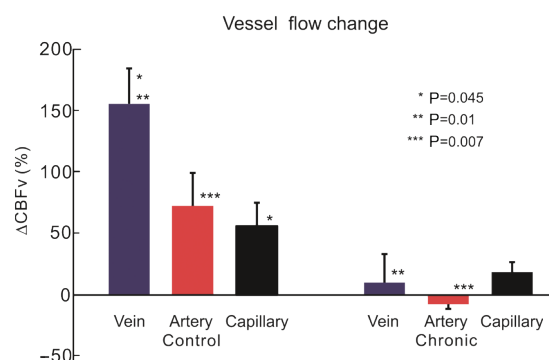


Figure 5 Cerebral blood flow velocity (CBFv) changes in vein, artery and capillary in control animals and cocaine animals. In control animals, the CBFv was increased to 154.4%±49%, 72.1%±26.6%, and 55.5%±32.8% in the vein, artery and capillary, respectively. However, in chronic cocaine the CBFv was changed 10%±39.9%, -7.5%±6.5%, and 18.4%±16.1% in the vein, artery and capillary, respectively. The CBFv of the big vessel (e.g., vein) was significant difference from capillary CBFv (P=0.045) in the control animals. The CBFv was significantly reduced by cocaine, e.g., P=0.017 for the vein and P=0.007 for the artery if comparing the CBFv changes with and without cocaine treatment.

circle, *Figure 3A1*) with the vasculature dilatation in the cortical window (red arrows, *Figure 4B1*), and it returned to normal afterwards (*Figure 4A2,A3*). This phenomenon was appeared in the mice in both animal groups above, thus confirming relevance to the inflammatory response to the surgery in the brain. Interestingly, although there was no obvious change in the morphology of the big vessels before and after the treatment of cocaine in the mouse (*Figure 4B0,B2,B3*), the capillaries seemed to be denser following the chronic treatment of cocaine (circled ROIs in *Figure 4B0-B3*). This is different from the control mouse above, which suggests the effect of cocaine on the microvascular network in the brain that can be explored by our μ OCA.

CBFv imaging of the cerebral vascular network within the cranial window of the brain, and the quantitative CBFv changes between the mice with and without cocaine exposure

Beside the μ OCA enables visualizing the cerebral vascular network as shown above, our OCT system can also detect the Doppler flow within these vessels simultaneously to provide the quantitative CBFv map of the brain (26,28).

In addition, with our PIM algorithm (29) the sensitivity of CBFv detection is enhanced to uncover capillary CBF embedded in the noise background (30). Furthermore, this technique allowed separation of arterial and venous branches and thus characterizing of their difference in response to stimuli such as cocaine.

Figure 3C0-C3 show the CBFv map of the control mouse at day 0, 3, 12 and 21 by μ ODT, and *Figure 4C0-C3* are the CBFv map also at day 0, 3, 12 and 21 but from a cocaine mouse instead. *Figure 5* summaries the quantitative CBFv change after the 21-day treatment (i.e., either by saline in control group or cocaine in chronic cocaine group) over its baseline (e.g., day 0-3) in the different type of vessels, including vein, artery and capillary.

As shown in *Figure 5*, the CBFv was increased in the control mouse brains over its baseline across all vascular trees in the post 21 days of the cranial window implantation. Specifically, the CBFv of the control mouse were increased to 154.4%±49.5%, 72.1%±26.6% and 55.5%±32.8% in the veins, arteries and capillaries, respectively, and there was no significant difference in CBFv changes between the veins and arteries (P=0.064). In contrast, in chronic cocaine group the percentage changes of CBFv in the veins, arteries and capillary were dramatically depressed. Specifically, the CBFv increases in the veins and capillaries were only 10.0%±39.9% and 18.5%±9.1%, respectively. In the arteries, the mean CBFv was changed to -7.5%±6.5% if comparing to its baseline, thus indicating the CBFv decrease in the vascular tree (including the capillary bed). The reduction of CBFv in the chronic cocaine animals reflected the vasoconstrictive effect of cocaine on the neurovascular network in the brain.

Dynamic CBFv changes in capillary bed induced by cocaine

Figure 6A illustrates the time traces of CBFv in the micro-vasculatures from day 0 (i.e., when the cranial window was implanted) to day 27 (i.e., 27 days after the implantation) in a control animal, in which the black lines represent the Δ CBFv of individual ROIs (control n=8) from the capillary bed in the various locations on the cortex within the cranial window whereas the red bold curve represents their averaged Δ CBFv of the capillaries as a function of time. As shown in *Figure 6A*, in day 3 of the post cranial window implantation, the capillary CBFv was varied, i.e., some of capillaries had the increase of CBFv about 26% and others decreased in the CBFv about 10-20%. However, this inhomogenous change in capillary CBFv

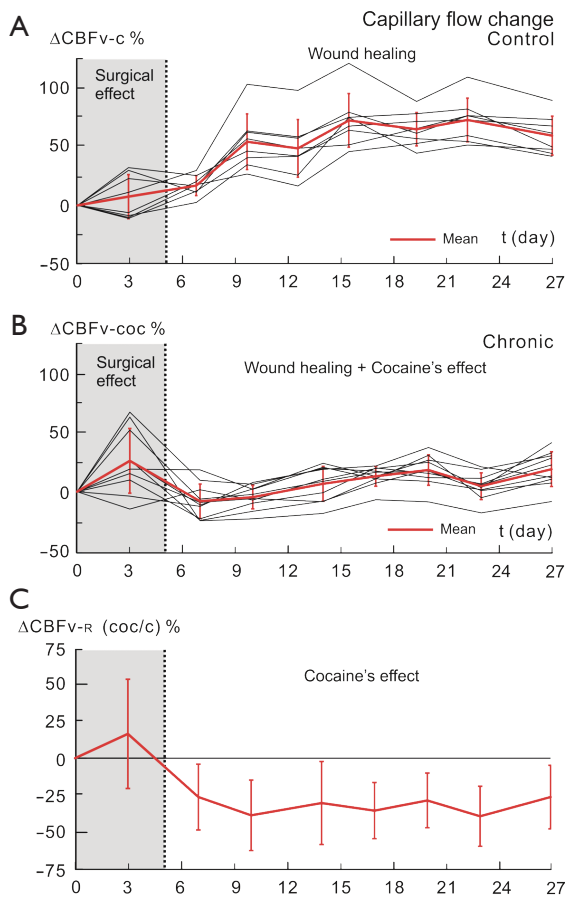


Figure 6 ΔCBFv of capillary in control group (A) and chronic cocaine group (B) and relative change of chronic cocaine data (C). (A) the ΔCBFv of each ROI was changed $7.0\% \pm 18\%$ on day 3 scan and the change was recovered by day 7. By day 16, the ΔCBFv was increased to $68\% \pm 21\%$ and maintained $56\text{--}61\% \pm 13\text{--}21\%$ until day 27; (B) mean of ΔCBFv increase and high deviation ($26.1\% \pm 27.3\%$) on day 3 and the ΔCBFv was decreased to $-8\% \pm 14.5\%$ by day 7 and then maintained around the range of $4\text{--}18\% \pm 8\text{--}14\%$; (C) the ratio between control and chronic cocaine data (ΔCBFv_R), showing ΔCBFv_R was decreased in response to cocaine by day 5 that reached to $-26\% \pm 22\%$ by day 10 and then maintained about $-38\% \pm 23\%$ until day 27. CBFv, cerebral blood flow velocity; ROI, region of interest.

was recovered around day 5 after the window implantation as being illustrated as grey strip in *Figure 6A*. Interestingly, from day 7 to day 15, the capillary CBFv was increasing as a function of time up to $68\% \pm 21\%$ over the baseline and it was plateaued at day 15 and kept it until day 27 of the post-surgery. This might indicate the capillary response to the wound healing process of the implantation on the cortex.

Figure 6B shows the dynamic CBFv changes in the capillary bed in the cocaine treated animal (ROIs $n=10$). Similarly to the control mouse, in day 3 of the surgical implantation of the cranial window on the cortex the inhomogenous change in capillary CBFv was observed (i.e., CBFv changes from -20% to 63% in the different capillary ROIs). This surgical effect was recovered by day 5 that is in agreement with the phenomenon observed in the control mouse above (*Figure 6A*). However on day 7, the capillary CBFv was decreased beyond the baseline about $8\% \pm 14\%$ followed by a plateau around this level during the recording period of the experiments (i.e., up to 27 days of the post implantation). This reflects a complex of the wound-healing process of the implantation with the cocaine's effects on the brain in the cocaine animal.

To extract the cocaine's effect from the complex with wound healing process of the surgical implantation on the brain in the chronic cocaine mouse, we computed the ratio of ΔCBFv in the capillaries between the cocaine mouse and the control mouse [i.e., shown as $\Delta\text{CBFv}_{\text{coc/c}}$ time trace, *Figure 6C*] shows the relative changes of mean $\Delta\text{CBFv}_{\text{coc/c}}$ over the baseline, i.e., $\text{CBFv}_{\text{coc/c}}(t) = \text{CBFv}_{\text{coc}}(t)/\text{CBFv}_{\text{c}}(t)$, $\Delta\text{CBFv}_R = \{[\text{CBFv}_{\text{coc/c}}(t_d) - \text{CBFv}_{\text{coc/c}}(t_0)]/\text{CBFv}_{\text{coc/c}}(t_0)\} \times 100$. The mean value of ΔCBFv_R was approximately unchanged during the day 0-5, thus indicating that the initial surgical effects on the capillary ΔCBFv was corrected. Furthermore, from day 5 on, the ΔCBFv_R was decreased gradually and reached to the maximal change to $-38\% \pm 23\%$ on day 10 of the post cocaine treatment. The low ΔCBFv_R value was maintained till the end of experimental recording on day 27. This decrease in capillary ΔCBFv_R were long and persistent over 27 days which is in agreement with the previous reports in animals (31) and human studies using other modalities such as PET and MRI, Doppler sonography (32,33). This demonstrates that the cocaine's effects on the microvascular CBF can be recovered from the complex with the wound healing process of the cranial window implantation, thus validating the surgical approach and the animal model above can be used for studying the microvascular changes and monitoring their development as a function of time along with a drug chronic treatment such as cocaine.

Discussion

Functional brain imaging has become an important tool in exploring both the healthy and dysfunctional brain in human and animals. Optical imaging allows

visualization of the vascular network of cortical brain at a high spatiotemporal resolution. OCT imaging techniques allow us to image 3D cerebrovascular networks, including artery, vein and capillary. Specifically, it can provide high resolution OCA of the cerebral network and quantitative CBFv within the individual vessels in the network, and also allow separation of arterial and venous branches and thus characterization of their differences in response to stimuli (e.g., cocaine).

To achieve the ability of imaging the brain for long term, we implanted a cranial window on the cortex of the animals in both control group (daily treated by saline) and cocaine group (daily cocaine administration). These mice were imaged periodically up to 27 days of the post window implantation by using multi-model imaging including the reflected-white light image, μ OCA and μ ODT. Our implantation surgery was successful and we did not have 'regrowing' of 'neomembrane' on the surface of the cortex as being reported previously (34,35). This might be because of the action of the immunosuppressive drugs (dexamethasone sodium phosphate) applied on the brain surface during the window implantation. This approach provides us the clear optical windows (*Figure 3A0-A3*, *Figure 4A0-A3*) to monitor the vasculature changes on the local cortex induced by the surgical preparation (*Figures 3,5*), as well to detect the hemodynamic response of neurovascular network to a stimulant such as cocaine (*Figures 4,5*). We have observed an initial short-term vasodilation with a minor and temporal bleeding within the first 2-3 days after the implantation, it returned to normal by day 5-6 in the post implantation. This phenomenon appeared in the groups of both control and cocaine animals (*Figure 6A,B*), thus indicating an inflammatory response of brain to the surgery (i.e., window implantation) which is in agreement with previous report from others (36). However, after day 7 of the implantation, the vasculature in the cortex became more in a 'wound-healing' process to increase the blood flow in the vascular tree (*Figures 5,6*). Importantly, in chronic cocaine animal group, the CBF changes were dramatically reduced across the entire vascular tree, including arteries, veins and capillaries (*Figure 5*). The reduction of CBFv in the chronic cocaine animals reflected the vasoconstrictive effect of cocaine on the neurovascular network in the brain.

With μ ODT, we enabled to capture CBFv in the capillaries and track their dynamic changes as a function of time in the control (*Figure 6A*) and cocaine (*Figure 6B*) animals. The inflammatory response as well 'wound-

healing process' were clearly observed in control mouse as demonstrated in *Figure 6A*. However, in cocaine mouse, besides the similar inflammatory response in the earlier period after the surgery, the CBFv in capillaries was depressed during the 'wound-healing process' period, thus indicating the complex of vascular physiology, i.e., competing the 'wound-healing response' (presumably increase in CBFv) with the constrict effect of cocaine (induced the decrease in CBFv). Fortunately, by using the dynamic changes of CBFv in the control animals, we were able to calibrate the CBFv changes induced by the 'wound healing', so that to explore the cocaine's effects on the capillary dynamics as illustrated in *Figure 6C*.

In summary, we have presented an approach of implanting a cranial window on mouse brain to achieve long-term cortical imaging, and we applied it to the animals with or without chronic cocaine exposure to valid the approach. We have observed vascular hemodynamic changes (i.e., vascular CBFv changes) induced by the cranial preparation which were appeared in the cortex with the implantations in both animals groups. By comparing with the control animals, the surgical related vascular physiology changes in the cortex can be calibrated, so that the cocaine-induced hemodynamic changes in the neurovasculature can be determined in the cocaine animals. Our results demonstrate that this methodology can be used on the animal model to explore the neurovascular functional changes induced by the brain diseases such as drug addiction.

Acknowledgements

This research was supported in part by NIH Grants K25-DA021200 (to C.D.), R21-DA032228 (to Y.P. and C.D.), and R01-DA029718 (to C.D. and Y.P.) and R01-NS084817 (to C.D.).

Disclosure: The authors declare no conflict of interest.

References

1. Bartzokis G, Beckson M, Lu PH, Edwards N, Rapoport R, Bridge P, Mintz J. Cortical gray matter volumes are associated with subjective responses to cocaine infusion. *Am J Addict* 2004;13:64-73.
2. Johnson BA, Devous MD Sr, Ruiz P, Ait-Daoud N. Treatment advances for cocaine-induced ischemic stroke: focus on dihydropyridine-class calcium channel

- antagonists. *Am J Psychiatry* 2001;158:1191-8.
3. Bolouri MR, Small GA. Neuroimaging of hypoxia and cocaine-induced hippocampal stroke. *J Neuroimaging* 2004;14:290-1.
 4. Büttner A, Mall G, Penning R, Sachs H, Weis S. The neuropathology of cocaine abuse. *Leg Med (Tokyo)* 2003;5 Suppl 1:S240-2.
 5. Zhang A, Cheng TP, Altura BT, Altura BM. Acute cocaine results in rapid rises in intracellular free calcium concentration in canine cerebral vascular smooth muscle cells: possible relation to etiology of stroke. *Neurosci Lett* 1996;215:57-9.
 6. Weissleder R, Pittet MJ. Imaging in the era of molecular oncology. *Nature* 2008;452:580-9.
 7. Drew PJ, Shih AY, Driscoll JD, Knutsen PM, Blinder P, Davalos D, Akassoglou K, Tsai PS, Kleinfeld D. Chronic optical access through a polished and reinforced thinned skull. *Nat Methods* 2010;7:981-4.
 8. Brown EB, Campbell RB, Tsuzuki Y, Xu L, Carmeliet P, Fukumura D, Jain RK. In vivo measurement of gene expression, angiogenesis and physiological function in tumors using multiphoton laser scanning microscopy. *Nat Med* 2001;7:864-8.
 9. Chaigneau E, Oheim M, Audinat E, Charpak S. Two-photon imaging of capillary blood flow in olfactory bulb glomeruli. *Proc Natl Acad Sci USA* 2003;100:13081-6.
 10. Vakoc BJ, Lanning RM, Tyrrell JA, Padera TP, Bartlett LA, Stylianopoulos T, Munn LL, Tearney GJ, Fukumura D, Jain RK, Bouma BE. Three-dimensional microscopy of the tumor microenvironment in vivo using optical frequency domain imaging. *Nat Med* 2009;15:1219-23.
 11. Srinivasan VJ, Jiang JY, Yaseen MA, Radhakrishnan H, Wu W, Barry S, Cable AE, Boas DA. Rapid volumetric angiography of cortical microvasculature with optical coherence tomography. *Opt Lett* 2010;35:43-5.
 12. Wang RK, Jacques SL, Ma Z, Hurst S, Hanson SR, Gruber A. Three dimensional optical angiography. *Opt Express* 2007;15:4083-97.
 13. An L, Qin J, Wang RK. Ultrahigh sensitive optical microangiography for in vivo imaging of microcirculations within human skin tissue beds. *Opt Express* 2010;18:8220-8.
 14. Kim SP, Simeral JD, Hochberg LR, Donoghue JP, Black MJ. Neural control of computer cursor velocity by decoding motor cortical spiking activity in humans with tetraplegia. *J Neural Eng* 2008;5:455-76.
 15. Wang RK, An L. Doppler optical micro-angiography for volumetric imaging of vascular perfusion in vivo. *Opt Express* 2009;17:8926-40.
 16. Jia Y, Grafe MR, Gruber A, Alkayed NJ, Wang RK. In vivo optical imaging of revascularization after brain trauma in mice. *Microvasc Res* 2011;81:73-80.
 17. Yuan Z, Chen B, Ren H, Pan Y. On the possibility of time-lapse ultrahigh-resolution optical coherence tomography for bladder cancer grading. *J Biomed Opt* 2009;14:050502.
 18. Fujimoto JG. Optical coherence tomography for ultrahigh resolution in vivo imaging. *Nat Biotechnol* 2003;21:1361-7.
 19. Goldey GJ, Roumis DK, Glickfeld LL, Kerlin AM, Reid RC, Bonin V, Schafer DP, Andermann ML. Removable cranial windows for long-term imaging in awake mice. *Nat Protoc* 2014;9:2515-38.
 20. Holtmaat A, Bonhoeffer T, Chow DK, Chuckowree J, De Paola V, Hofer SB, Hübener M, Keck T, Knott G, Lee WC, Mostany R, Mrcic-Flogel TD, Nedivi E, Portera-Cailliau C, Svoboda K, Trachtenberg JT, Wilbrecht L. Long-term, high-resolution imaging in the mouse neocortex through a chronic cranial window. *Nat Protoc* 2009;4:1128-44.
 21. Shih AY, Driscoll JD, Drew PJ, Nishimura N, Schaffer CB, Kleinfeld D. Two-photon microscopy as a tool to study blood flow and neurovascular coupling in the rodent brain. *J Cereb Blood Flow Metab* 2012;32:1277-309.
 22. Hof PR, Young WG, Bloom FE, Belichenko PV, Celio MR. eds. *Comparative Cytoarchitectonic Atlas of the C57BL/6 and 129/Sv Mouse Brains*. New York: Elsevier, 2000.
 23. Paxinos G, Franklin KB. eds. *The Mouse Brain in Stereotaxic Coordinates, Second Edition*. San Diego: Academic Press, 2004.
 24. Pan YT, Wu ZL, Yuan ZJ, Wang ZG, Du CW. Subcellular imaging of epithelium with time-lapse optical coherence tomography. *J Biomed Opt* 2007;12:050504.
 25. Mariampillai A, Standish BA, Moriyama EH, Khurana M, Munce NR, Leung MK, Jiang J, Cable A, Wilson BC, Vitkin IA, Yang VX. Speckle variance detection of microvasculature using swept-source optical coherence tomography. *Opt Lett* 2008;33:1530-2.
 26. Zhao Y, Chen Z, Saxer C, Xiang S, de Boer JF, Nelson JS. Phase-resolved optical coherence tomography and optical Doppler tomography for imaging blood flow in human skin with fast scanning speed and high velocity sensitivity. *Opt Lett* 2000;25:114-6.
 27. Yuan Z, Luo Z, Volkow ND, Pan Y, Du C. Imaging separation of neuronal from vascular effects of cocaine on rat cortical brain in vivo. *Neuroimage* 2011;54:1130-9.

28. Srinivasan VJ, Atochin DN, Radhakrishnan H, Jiang JY, Ruvinskaya S, Wu W, Barry S, Cable AE, Ayata C, Huang PL, Boas DA. Optical coherence tomography for the quantitative study of cerebrovascular physiology. *J Cereb Blood Flow Metab* 2011;31:1339-45.
29. Ren H, Du C, Yuan Z, Park K, Volkow ND, Pan Y. Cocaine-induced cortical microischemia in the rodent brain: clinical implications. *Mol Psychiatry* 2012;17:1017-25.
30. Pan Y, You J, Volkow ND, Park K, Du C. Ultrasensitive detection of 3D cerebral microvascular network dynamics in vivo. *Neuroimage* 2014;103:492-501.
31. Perles-Barbacaru TA, Procissi D, Demyanenko AV, Hall FS, Uhl GR, Jacobs RE. Quantitative pharmacologic MRI: mapping the cerebral blood volume response to cocaine in dopamine transporter knockout mice. *Neuroimage* 2011;55:622-8.
32. Volkow ND, Mullani N, Gould KL, Adler S, Krajewski K. Cerebral blood flow in chronic cocaine users: a study with positron emission tomography. *Br J Psychiatry* 1988;152:641-8.
33. Herning RI, King DE, Better WE, Cadet JL. Neurovascular deficits in cocaine abusers. *Neuropsychopharmacology* 1999;21:110-8.
34. Roe AW. Long-term optical imaging of intrinsic signals in anesthetized and awake monkeys. *Appl Opt* 2007;46:1872-80.
35. Chen LM, Friedman RM, Roe AW. Optical imaging of digit topography in individual awake and anesthetized squirrel monkeys. *Exp Brain Res* 2009;196:393-401.
36. Hammer DX, Lozzi A, Abliz E, Greenbaum N, Agrawal A, Krauthamer V, Welle CG. Longitudinal vascular dynamics following cranial window and electrode implantation measured with speckle variance optical coherence angiography. *Biomed Opt Express* 2014;5:2823-36.

Cite this article as: Park K, You J, Du C, Pan Y. Cranial window implantation on mouse cortex to study microvascular change induced by cocaine. *Quant Imaging Med Surg* 2015;5(1):97-107. doi: 10.3978/j.issn.2223-4292.2014.11.31